Low-velocity impact analysis of laminated composite plates and shells with generalized differential quadrature method

Hasan Kurtaran[1*]

[1] *Adana Alparslan Turkes Science and Technology University, Engineering Faculty, Mechanical Engineering, Adana*

Abstract

In this article, low-velocity impact analysis of laminated composite plates and shells for small and large displacements is investigated using Generalized Differential Quadrature (GDQ) method. Equation of motion for impact system is derived using virtual work principle. First-order shear deformation theory (FOST) is employed to consider transverse shear effects and Von-Karman nonlinear strain-displacement relationships are used in large displacement analyses. Spatial derivatives are expressed with GDQ method and time integration of dynamic equations is performed using Newmark average acceleration method. Several laminated composite impact problems from the literature are solved with the proposed method. Very close results are obtained with the literature using only limited number of grids, showing the efficiency of the method in contact-impact problems.

Tabakalı kompozit levha ve kabukların genelleştirilmiş diferansiyel kuadrature metodu ile düşük çarpma hızlarındaki analizleri

Özet

Bu çalışmada tabakalı kompozit levha ve panellerin düşük çarpma hızlarındaki nonlineer dinamik davranışı Genelleştirilmiş Diferansiyel Kuadrature (Generalized Differential Quadrature) yöntemi ile incelenmektedir. Sistemin dinamik denklemleri Virtüel iş ilkesi ile elde edilmektedir. Düzleme dik doğrultudaki kalınlık etkisi 1. mertebe kayma deformasyon teorisi ile dikkate alınmaktadır. Büyük yer değiştirmeler Von-Karman nonlineer birim şekil değişimleri ile dikkate alınmaktadır. Konumsal türevler Genelleştirilmiş Diferansiyel Quadrature yöntemi ile zaman integrasyonu da Newmark metodu ile hesaplanmaktadır. Önerilen metotla birçok çarpma problemi çözülmüş ve literatürdeki sonuçlarla karşılaştırılmıştır. Önerilen metodun çarpma problemlerinin incelenmesinde etkili ve verimli bir yöntem olduğu gösterilmiştir.

[*]Sorumlu yazar (Corresponding author): Hasan Kurtaran, hasan@atu.edu.tr

Low-velocity impact analysis of laminated composite plates and shells with generalized differential quadrature method

1. Introduction

Composite materials are increasingly used in aerospace, civil, automotive, marine and other industries due to its light-weight feature and high strength-to-weight ratio. Composite structures may face to low-velocity impacts such as dropped tools during maintenance. Therefore, understanding the dynamic behavior of these structures is very important to enable safe and economical designs as well as to prepare an appropriate maintenance program.

Different analytical and numerical methods were used in determining impact response of composite plates and shells. For example, Karas [1] obtained analytical solution for impact response of isotropic plates. Chen and Sun [2] analyzed large deflection impact response of composite plates using Finite Element Method (FEM). They used Mindlin plate theory and 9-node isoparametric quadrilateral plate element. Sun and Chen [3] carried out small deflection response of initially stressed composite plates using FEM. Wu and Chang [4] conducted small deflection impact analysis of laminated composite plates using 8-node brick element in FEM. Cairns and Lagace [5] investigated the influence of different parameters on the impact behavior of composite plates analytically using Rayleigh-Ritz method. Liou [6] established contact law for carbon-epoxy laminated composite plates and conducted impact analysis using FEM. Chun and Lam [7] analyzed dynamic behavior of laminated composite plates under low velocity impact using mode shapes and transformation of principal. They used Reddy's higher-order shear deformation theory to take transverse strain into account. Vaziri et al. [8] obtained transient response of laminated composite plates and cylindrical shells subjected to impact using a super finite element method. Karmakar and Sinha [9] analyzed dynamic behavior of laminated composite pre-twisted rotating plates using FEM. Her and Liang [10] obtained impact response of laminated composite cylindrical and spherical shells. They compared FEM results with analytical solution. Choi and Lim [11] performed low-velocity impact analysis of composite plates analytically through linearized contact law. Karmakar and Kishimoto [12] investigated impact behavior of delaminated composite rotating shallow shells using FEM by calculating contact force with modified Hertzian contact law. Tiberkak et al. [13] investigated damage prediction in composite plates under low velocity impact using FEM. Kumar [14] analyzed large deformation impact response of composite cylindrical shells with FEM considering material degradation effect during impact. Khalili et al. [15] investigated FEM approach for impact of composite cylindrical tubes. Dey and Karmakar [16] predicted dynamic response of delaminated composite conical shells under oblique impact using FEM. Park [17] investigated low-velocity impact behavior of graphite/epoxy composite and steel plates for different impactor masses using FEM. Mao et al. [18] predicted dynamic response and damage analysis of laminated composite plates under low-velocity oblique impact analytically. Rout and Karmakar [19] analyzed low velocity impact behavior of delaminated composite stiffened shells using FEM. Analytical methods for impact problems of composite plates are included in detail in the related book of [20].

As an efficient numerical method, using less grid points with acceptable accuracy, Differential Quadrature Method (DQM) was introduced by Bellman et al. in the early 1970s [21, 22] and developed by Shu [23]. Nowadays, improved form of DQM is known as Generalized Differential Quadrature (GDQ) method. For detailed and complete information about the evolution of GDQ method and its application in various forms in the solution of engineering problems, reader is referred to the related books and review articles [23-27]. GDQ method was successfully used in dynamic analysis of plates and shells with various material properties [28-35].

From the literature survey, it is seen that GDQ method has not been yet used in predicting impact behavior of laminated composite structures. Therefore, in this study GDQ method is applied to

efficiently predict the transient response of laminated composite plates and shells under low-velocity impacts. In the following sections, dynamic equations for composite shells are derived using virtual work principle. Partial derivatives in the equation of motion are expressed with GDQ method and time integration is carried out using Newmark average acceleration method. Several impact problems related to laminated composite plates and shells are solved with the proposed method and compared with the literature to show its efficiency.

2. Governing equations

2.1. Constitutive equations

In this section, constitutive equations for laminated composite cylindrical panels are derived. Geometrical parameters of a cylindrical panel in a curvilinear coordinate system is shown in Fig. 1. In Fig. 1, x and y denote the lines of curvature on the middle surface ($z = 0$).
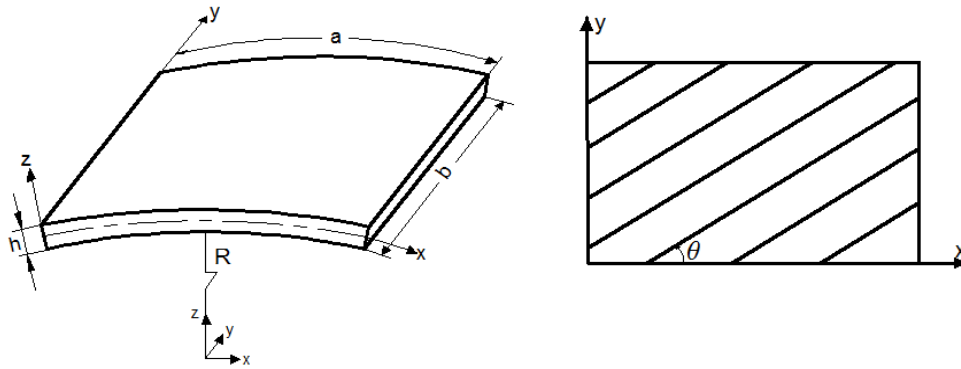
Figure 1. Cylindrical panel

Displacements of a general point (x, y, z) at a time t based on FOST theory can be written as

$$u(x,y,z,t) = u_0(x,y,t) + z\theta_x(x,y,t)$$

$$v(x,y,z,t) = v_0(x,y,t) + z\theta_y(x,y,t) \qquad (1)$$

$$w(x,y,z,t) = w_0(x,y,t)$$

where u_0, v_0, w_0 correspond to mid-plane displacements. θ_x and θ_y correspond to the rotations about y and x axes respectively.

Large displacement strains for cylindrical panel are expressed as following [36]:

$$\varepsilon = \begin{Bmatrix} \varepsilon_x \\ \varepsilon_y \\ \gamma_{xy} \\ \gamma_{yz} \\ \gamma_{zx} \end{Bmatrix} = \begin{Bmatrix} \dfrac{\partial u_0}{\partial x} + \dfrac{w_0}{R} + \dfrac{1}{2}\left(\dfrac{\partial w_0}{\partial x}\right)^2 \\[2mm] \dfrac{\partial v_0}{\partial y} + \dfrac{1}{2}\left(\dfrac{\partial w_0}{\partial y}\right)^2 \\[2mm] \dfrac{\partial u_0}{\partial y} + \dfrac{\partial v_0}{\partial x} + \dfrac{\partial w_0}{\partial x}\dfrac{\partial w_0}{\partial y} \\[2mm] \theta_y + \dfrac{\partial w_0}{\partial y} \\[2mm] \theta_x + \dfrac{\partial w_0}{\partial x} - \dfrac{v_0}{R} \end{Bmatrix} + z \begin{Bmatrix} \dfrac{\partial \theta_x}{\partial x} \\[2mm] \dfrac{\partial \theta_y}{\partial y} \\[2mm] \dfrac{\partial \theta_x}{\partial y} + \dfrac{\partial \theta_y}{\partial x} \\[2mm] 0 \\[2mm] 0 \end{Bmatrix} \tag{2}$$

where R is cylindrical panel radius in *x-z* plane. In the case of small displacements, nonlinear terms of $\frac{1}{2}\left(\frac{\partial w_0}{\partial x}\right)^2$, $\frac{1}{2}\left(\frac{\partial w_0}{\partial y}\right)^2$ and $\frac{\partial w_0}{\partial x}\frac{\partial w_0}{\partial y}$ are dropped in Eq. (2).

The constitutive equation for laminated composite cylindrical shell panel can be written in terms of in-plane force and moment resultants as

$$\begin{Bmatrix} N_x \\ N_y \\ N_{xy} \\ M_x \\ M_y \\ M_{xy} \end{Bmatrix} = \begin{bmatrix} A_{11} & A_{12} & A_{16} & B_{11} & B_{12} & B_{16} \\ A_{12} & A_{22} & A_{26} & B_{12} & B_{22} & B_{26} \\ A_{16} & A_{26} & A_{66} & B_{16} & B_{26} & B_{66} \\ B_{11} & B_{12} & B_{16} & D_{11} & D_{12} & D_{16} \\ B_{12} & B_{22} & B_{26} & D_{12} & D_{22} & D_{26} \\ B_{16} & B_{26} & B_{66} & D_{16} & D_{26} & D_{66} \end{bmatrix} \begin{Bmatrix} \dfrac{\partial u_0}{\partial x} + \dfrac{w_0}{R} + \dfrac{1}{2}\left(\dfrac{\partial w_0}{\partial x}\right)^2 \\[2mm] \dfrac{\partial v_0}{\partial y} + \dfrac{1}{2}\left(\dfrac{\partial w_0}{\partial y}\right)^2 \\[2mm] \dfrac{\partial u_0}{\partial y} + \dfrac{\partial v_0}{\partial x} + \dfrac{\partial w_0}{\partial x}\dfrac{\partial w_0}{\partial y} \\[2mm] \dfrac{\partial \theta_x}{\partial x} \\[2mm] \dfrac{\partial \theta_y}{\partial y} \\[2mm] \dfrac{\partial \theta_x}{\partial y} + \dfrac{\partial \theta_y}{\partial x} \end{Bmatrix} \tag{3}$$

Laminate constitutive equation for transverse shear in terms of shear force resultant is written as

$$\begin{Bmatrix} Q_y \\ Q_x \end{Bmatrix} = \begin{bmatrix} A_{44} & A_{45} \\ A_{45} & A_{55} \end{bmatrix} \begin{Bmatrix} \gamma_{yz} \\ \gamma_{zx} \end{Bmatrix} \tag{4}$$

A_{ij}, B_{ij}, D_{ij} in Eqs. 3-4 correspond to laminate stiffness coefficients for in-plane, bending stretching coupling, bending and transverse shear stiffness and are calculated as

$$\left\{ A_{ij}, B_{ij}, D_{ij} \right\} = \sum_{k=1}^{n} \int_{z_{k-1}}^{z_k} \left\{ 1, z, z^2 \right\} \overline{Q}_{ij}^{(k)} \, dz \qquad (i, j = 1,2,6) \tag{5}$$

$$A_{ij} = \sum_{k=1}^{n} k_i k_j \int_{z_{k-1}}^{z_k} \overline{Q}_{ij}^{(k)} \, dz \qquad (i, j = 4,5) \tag{6}$$

where $k_i^2 = 5/6$ (i=4,5) denote the shear correction factor. $\overline{Q}_{ij}^{(k)}$ indicates the transformed stiffness coefficients of k-th layer.

Mass inertias for laminate are written as

$$\left\{ I_0, I_1, I_2 \right\} = \sum_{k=1}^{n} \int_{z_{k-1}}^{z_k} \left\{ 1, z, z^2 \right\} \rho^{(k)} dz \tag{7}$$

where $\rho^{(k)}$ is the density of the k-th layer.

2.2. Virtual work equation

In this section, equation of motion is derived for a composite panel under mass impact using dynamic version of the virtual work principle. Description of contact procedure between a laminated plate and a spherical ball made of isotropic material is shown in Fig. 2.
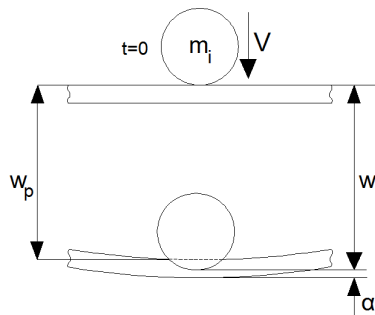
Figure 2. Description of contact-ımpact system

Low-velocity impact analysis of laminated composite plates and shells with generalized differential quadrature method

Virtual work principle for cylindrical shell panel in the absence of damping can be expressed as [7].

$$\sum_{k=1}^{L}\int_{z_{k-1}}^{z_k}[\int_{\Omega}\{\sigma_x^{(k)}\delta\varepsilon_x+\sigma_y^{(k)}\delta\varepsilon_y+\tau_{xy}^{(k)}\delta\gamma_{xy}+\tau_{yz}^{(k)}\delta\gamma_{yz}+\tau_{zx}^{(k)}\delta\gamma_{zx}$$

$$+\rho^{(k)}\left[\left(\ddot{u}_0+z\ddot{\theta}_x\right)(\delta u_0+z\delta\theta_x)+\left(\ddot{v}_0+z\ddot{\theta}_y\right)(\delta v_0+z\delta\theta_y)+\ddot{w}_0\,\delta w_0\right]\}dxdy]dz \tag{8}$$

$$=-F_c\delta\alpha$$

In Eq. (8), F_c indicates the contact force between the impactor mass and the target panel. α is the indentation of the target panel. Eq. (8) can be rewritten using force and moment resultants and mass inertias as below

$$\int_{\Omega}[N_x\delta\varepsilon_x^0+N_y\delta\varepsilon_y^0+N_{xy}\delta\gamma_{xy}^0+M_x\delta\varepsilon_x^0+M_y\delta\varepsilon_y^0+M_{xy}\delta\gamma_{xy}^0+Q_y\delta\gamma_{yz}^0$$

$$+Q_x\delta\gamma_{zx}^0+(I_0\ddot{u}_0+I_1\ddot{\theta}_x)\delta u_0+(I_0\ddot{v}_0+I_1\ddot{\theta}_y)\delta v_0+I_1\ddot{w}_0\,\delta w_0+(I_1\ddot{u}_0+I_2\ddot{\theta}_x)\delta\theta_x \tag{9}$$

$$+(I_1\ddot{v}_0+I_2\ddot{\theta}_y)\delta\theta_y]dxdy=-F_c\delta\alpha$$

Equation of motion for cylindrical panel can be shortly written in matrix form as

$$M\ddot{U}+P=F(F_c) \tag{10}$$

where M is mass matrix and F, P, $\ddot{U}$ are external force vector that includes contact force, internal force and acceleration vectors respectively.

Equation of motion for impactor mass is written as

$$m_i\ddot{w}_i=F_c \tag{11}$$

where m_i and $\ddot{w}_i$ indicate the mass and acceleration of the impactor respectively. Equations of motion for cylindrical panel and impactor mass can be combined as following

$$\begin{bmatrix} M & 0 \\ 0 & m_i \end{bmatrix} \begin{Bmatrix} \ddot{U} \\ \ddot{w}_i \end{Bmatrix} + \begin{Bmatrix} P \\ 0_i \end{Bmatrix} = \begin{Bmatrix} F(F_c) \\ F_c \end{Bmatrix} \tag{12}$$

Eq. (12) can be rewritten as a single matrix equation as

$$\bar{M}\ddot{W} + \bar{P} = \bar{F} \tag{13}$$

Contact force F_c can be calculated using a modified nonlinear Hertzian indentation law [2] as

$$F_c = \begin{Bmatrix} k\alpha^{1.5} & for & loading \\ F_m\left(\dfrac{\alpha - \alpha_0}{\alpha_m - \alpha_0}\right)^{2.5} & for & unloading \\ F_m\left(\dfrac{\alpha - \alpha_0}{\alpha_m - \alpha_0}\right)^{1.5} & for & reloading \end{Bmatrix} \tag{14}$$

$$\alpha_0 = \begin{Bmatrix} \beta(\alpha_m - \alpha_{cr}) & if & \alpha_m > \alpha_{cr} \\ 0 & if & \alpha_m <= \alpha_{cr} \end{Bmatrix} \tag{15}$$

Regarding coefficients in Eqs.12-13, k is the contact stiffness, F_m is the maximum impact force reached before unloading, α_m is the maximum indentation depth, α_0 is the permanent indentation depth in the target panel. β=0.094 and α_{cr}=1.667x10^{-4} m values are commonly used in the impact analyses in the literature [3]. Contact deformation i.e. indentation is defined as

$$\alpha = w_i - w_p \tag{16}$$

where w_i is the displacement of the impactor and w_p is the displacement of the panel at the impact point.

The Hertzian contact stiffness k for-panel-impactor system is given as [10, 18]

$$k = \frac{4}{3}\sqrt{\frac{R_1 R}{R_1 + R}} \frac{1}{\left(1 - v_i^2\right)/E_i + \left(1 - v_p^2\right)/E_p}$$ (17)

where R, E_p, v_p denote radius, elastic modulus and poisson ratio of impacted panel in transverse direction. R, E_i, v_i denote radius, elastic modulus and poisson ratio of the impactor mass.

2.3. Geometric mapping

Integrals in the equation of motion can be calculated easily using numerical methods such as Gauss quadrature or Gauss Lobatto quadrature rules. To do that, cartesian domain is often transformed into a bi-unit square domain as shown in Fig. 3 using geometric mapping as below:
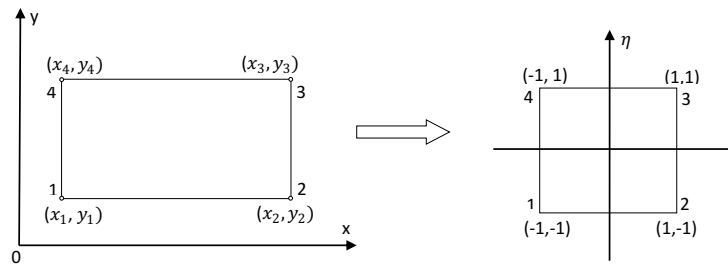
Figure 3. Geometric mapping from cartesian to natural coordinates

$$x(\xi,\eta) = \sum S_k(\xi,\eta)x_k \qquad -1 \leq \xi \leq 1$$ (18a)

$$y(\xi,\eta) = \sum S_k(\xi,\eta)y_k \qquad -1 \leq \eta \leq 1$$ (18b)

In Eq. (16), $S_k(\xi,\eta)$ correspond to interpolation functions and ξ, η indicate natural coordinates for bi-unit square domain.

Partial derivatives of a function $f(x,y)$ in cartesian domain can be expressed in terms of natural coordinates as:

$$\frac{\partial f}{\partial x} = \frac{1}{J}\left(\frac{\partial y}{\partial \eta}\frac{\partial f}{\partial \xi} - \frac{\partial y}{\partial \xi}\frac{\partial f}{\partial \eta}\right)$$ (19)

$$\frac{\partial f}{\partial y} = \frac{1}{J}\left(\frac{\partial x}{\partial \xi}\frac{\partial f}{\partial \eta} - \frac{\partial x}{\partial \eta}\frac{\partial f}{\partial \xi}\right)$$ (20)

where *J* indicates the determinant of the Jacobian and it is given as

$$J = \frac{\partial x}{\partial \xi}\frac{\partial y}{\partial \eta} - \frac{\partial y}{\partial \xi}\frac{\partial x}{\partial \eta} \tag{21}$$

3. Generalized differential quadrature method

In this study, GDQ method is employed in the calculation of spatial derivatives at pre-determined grid points as shown in Fig. 4. In GDQ method, derivative of a function with respect to a variable at a given discrete point can be calculated as a weighted linear sum of the function values at all discrete points in the mesh line [31].
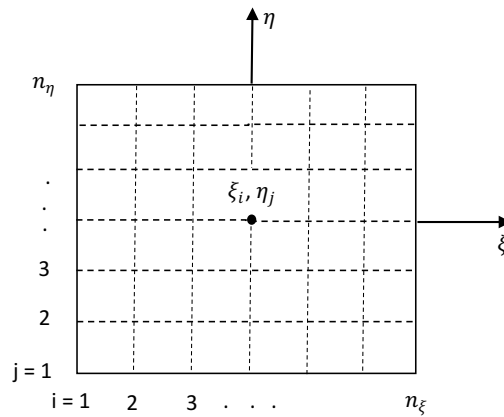
Figure 4. Grid points in two dimensional natural coordinate system

In GDQ method, *r*-th order derivative of a function *f*(ξ) with *n* discrete grid points is stated as

$$\left(\frac{\partial f^r(x)}{\partial \xi^r} \right)_{\xi_i} = \sum_{j=1}^{n} C_{ij}^{(r)} f_j \tag{22}$$

where ξ_i denote the discrete points, f_j and $C_{ij}^{(r)}$ correspond to the function values at these points and related weighting coefficients, respectively. Accuracy of GDQ method is highly affected by the choice of weight coefficients as well as the location and number of grid points.

In GDQ method, Lagrange polynomial functions are used in determining the weight coefficients $C_{ij}^{(r)}$. Weight coefficients for first-order derivative, i.e. *r*=1, can be written as

$$C_{ij}^{(1)} = \frac{\Phi(\xi_i)}{(\xi_i - \xi_j)\Phi(\xi_j)} \qquad (i \neq j) \tag{23}$$

where

$$\Phi(\xi_i) = \prod_{j=1}^{n} (\xi_i - \xi_j) \quad (i \neq j)$$

(24)

Higher-order derivatives can be obtained through recursive relations as below:

$$C_{ij}^{(r)} = r \left[C_{ii}^{(r-1)} C_{ij}^{(1)} - \frac{C_{ij}^{(r-1)}}{(\xi_i - \xi_j)} \right] \quad (i \neq j)$$

(25)

$$C_{ii}^{(r)} = -\sum_{\substack{j=1 \\ i \neq j}}^{n} C_{ij}^{(r)}$$

(26)

One dimensional derivatives can be extended to the calculation of partial derivatives in GDQ method. Considering Fig. 4 where n_ξ and n_η denote grid numbers in ξ and η directions respectively, partial derivatives at a point (ξ_i, η_j) can be written as below:

$$\left(\frac{\partial f^r(\xi, \eta)}{\partial \xi^r} \right)_{\xi_i, \eta_j} = \sum_{k=1}^{n_x} C_{kj}^{(r)} f_{kj}$$

(27)

$$\left(\frac{\partial f^s(\xi, \eta)}{\partial \eta^s} \right)_{\xi_i, \eta_j} = \sum_{m=1}^{n_y} C_{im}^{(s)} f_{im}$$

(28)

$$\left(\frac{\partial f^{(r+s)}(\xi, \eta)}{\partial \xi^r \partial \eta^s} \right)_{\xi_i, y_j} = \frac{\partial^r}{\partial \xi^r} \left(\frac{\partial^s f}{\partial \eta^s} \right) = \sum_{k=1}^{n_x} C_{kj}^{(r)} \sum_{m=1}^{n_y} C_{im}^{(s)} f_{km}$$

(29

where *r* and *s* are order of partial derivatives.

Cartesian derivatives can be expressed in terms of derivatives in natural coordinates as

$$\left(\frac{\partial f}{\partial x} \right)_{ij} = \frac{1}{J_{ij}} \left[\left(\frac{\partial y}{\partial \eta} \right)_{ij} \left(\sum_{k=1}^{n_x} C_{kj}^{(1)} f_{kj} \right) - \left(\frac{\partial y}{\partial \xi} \right)_{ij} \left(\sum_{m=1}^{n_y} C_{im}^{(1)} f_{im} \right) \right]$$

(30)

$$\left(\frac{\partial f}{\partial y}\right)_{ij} = \frac{1}{J_{ij}}\left[\left(\frac{\partial x}{\partial \xi}\right)_{ij}\left(\sum_{m=1}^{n_y} C_{im}^{(1)} f_{im}\right) - \left(\frac{\partial x}{\partial \eta}\right)_{ij}\left(\sum_{k=1}^{n_x} C_{kj}^{(1)} f_{kj}\right)\right] \qquad (31)$$

In discretization of spatial domain, Gauss-Lobatto points are chosen as grid points in this study. These points are also utilized in numerical integration of Eq. (9). Lobatto rule creates non-uniform grid points which increase the accuracy of derivatives in GDQ method. Moreover, Gauss-Lobatto rule can locate grid points on the boundaries simplifying the application of boundary conditions.

4. Solution of equation of motion

Time integration of equation of motion of impact system can be carried out using implicit Newmark constant average acceleration time integration scheme. In Newmark method equation of motion for impact system is expressed at $(n+1)$-th time step, i.e at time $(n+1)\Delta t$ or t_{n+1} as

$$\bar{M}\ddot{W}_{n+1} + \bar{P}_{n+1} = \bar{F}_{n+1} \qquad (32)$$

Substituting the following acceleration and velocity expressions at t_{n+1} in Eq. (32)

$$\ddot{W}_{n+1} = C_0\left(W_{n+1} - W_n\right) - C_1\dot{W}_n - \ddot{W}_n \qquad (33)$$

$$\dot{W}_{n+1} = \dot{W}_n + \Delta t\ddot{W}_n + \frac{\Delta t}{2}\left(\ddot{W}_{n+1} - \ddot{W}_n\right) \qquad (34)$$

Following algebraic equation system in terms of unknown displacements are obtained

$$C_0\bar{M}W_{n+1} + \bar{P}_{n+1} = \bar{F}_{n+1} + \bar{M}(C_0W_n + C_1\dot{W}_n + \ddot{W}_n) \qquad (35)$$

where $C_0 = 4/\Delta t^2$ and $C_1 = 4/\Delta t$ can be used.

Eq. (35) is nonlinear since internal force vector $\bar{P}_{n+1}$ and external force vector $\bar{F}_{n+1}$ are nonlinear function of unknown displacement vector W_{n+1}. In the case of small displacement Eq. (35) is still nonlinear due to contact force definition given in Eq. 14. An iterative approach such as Newton-Raphson method can be employed for the solution of Eq. (35). In Newton-Raphson solution, Eq. (35) is expressed in terms of error function or residual forces R_{n+1} as

$$R_{n+1} = \bar{F}_{n+1} + \bar{M}(C_0W_n + C_1\dot{W}_n + \ddot{W}_n) - C_0\bar{M}W_{n+1} - \bar{P}_{n+1} \qquad (36)$$

Improved solution for W_{n+1}^{i+1} at $i+1$-th iteration can be obtained using Taylor series expansion of R_{n+1}^{i+1} in terms of known values at i-th iteration and equating it to zero as

Low-velocity impact analysis of laminated composite plates and shells with generalized differential quadrature method

$$R_{n+1}^{i+1} \approx R_{n+1}^{i} + K_{n+1}^{i}(W_{n+1}^{i+1} - W_{n+1}^{i}) = 0 \tag{37}$$

where K_{n+1}^{i} corresponds to tangent stiffness matrix. Eq. (37) can be expressed in incremental form as

$$K_{n+1}^{i} \Delta W_{n+1}^{i} = -R_{n+1}^{i} \tag{38}$$

where ΔW_{n+1}^{i} denotes the displacement increment in the current iteration and is given as

$$\Delta W_{n+1}^{i} = W_{n+1}^{i+1} - W_{n+1}^{i} \tag{39}$$

Improved solution at (*i*+1)-th iteration is written as

$$W_{n+1}^{i+1} = W_{n+1}^{i} + \Delta W_{n+1}^{i} \tag{40}$$

Iterations are repeated until the error function R_{n+1}^{i+1} is sufficiently close to zero. Initial accelerations $\ddot{W}_0$ in the first iteration are obtained by using initial displacements W_0 and velocities $\dot{W}_0$ at time *t*=0.

5. Examples

A Matlab code is written to solve contact impact problems using GDQ method. The code is first validated with an isotropic plate impact problem and then used to solve several laminated composite plate and shell panel problems from the literature. In the solution of all problems in this study, grid numbers in all directions are chosen as odd numbers in order to locate a grid point at the mesh/panel center. After solutions, time history for center transverse deflection and velocity as well as contact force are compared with those in the literature. Unless otherwise stated, plate and shell structures are impacted by the impactor at the center and contact stiffness *k* is calculated by Eq. (17).

5.1. Isotropic plate impact problem

In this validation example, a steel plate is impacted by a rigid ball. Plate is simply supported at all edges. Plate dimensions are: *a*=0.2 m, *b*=0.2 m and thickness *h*=0.008 m. Material properties are: *E*=206 GPa, *v*=0.3, ρ=7860 kg/m^3. Ball is made up of steel and material properties are taken the same as with plate. Radius and initial velocity of steel ball is given as Ri=0.01 m and V0=-1 m/s respectively. Dynamic equations are solved with GDQ method. In the solution, time step value of Δt=1 μs is used. After solution, contact force, transverse displacements and velocities of the plate and ball are compared with those in the literature as shown in Figs. 5-8 [1, 4, 7, 10]. In Figs. 5-8, Karas [1] predicts response using series and small-time increment method. Wu and Chang obtain results with FEM where they used 8-node brick elements with incompatible modes. Wu and Chang do not mention about the mesh size in their article. However, in the article of Her and Liang [10], it is mentioned that Karas solution is converged using 80x80x2 solid element mesh using commercial FEM code ANSYS/LS-DYNA. Chun and Lam calculate the response using mode summation method where they used 49 terms in series expansion in each direction. From comparison of results in Figs. 5-8, very good agreement is observed

with the literature using only 9x9 grid numbers in *x* and *y* directions. This validates the accuracy of the developed impact code.
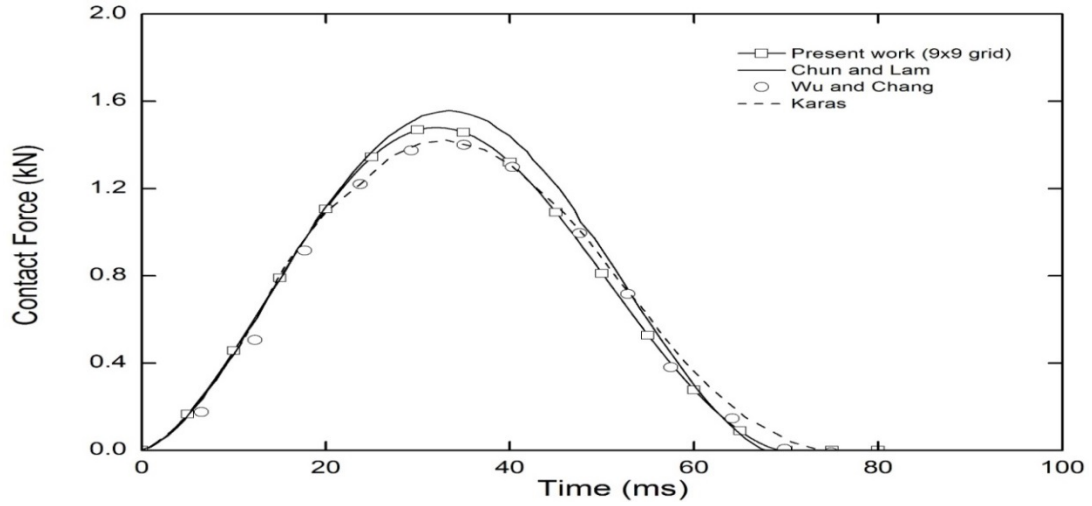
Figure 5. Comparison of contact force
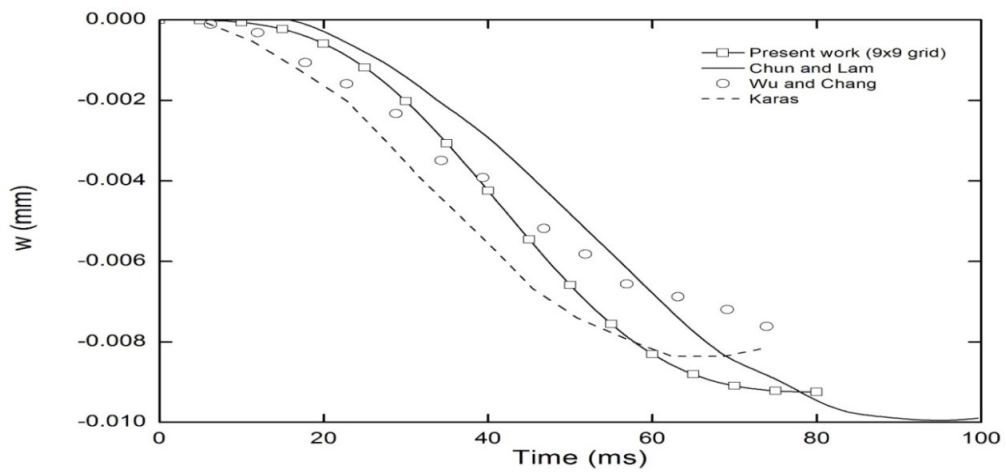
Figure 6. Comparison of the transverse displacement of the plate at the contact point
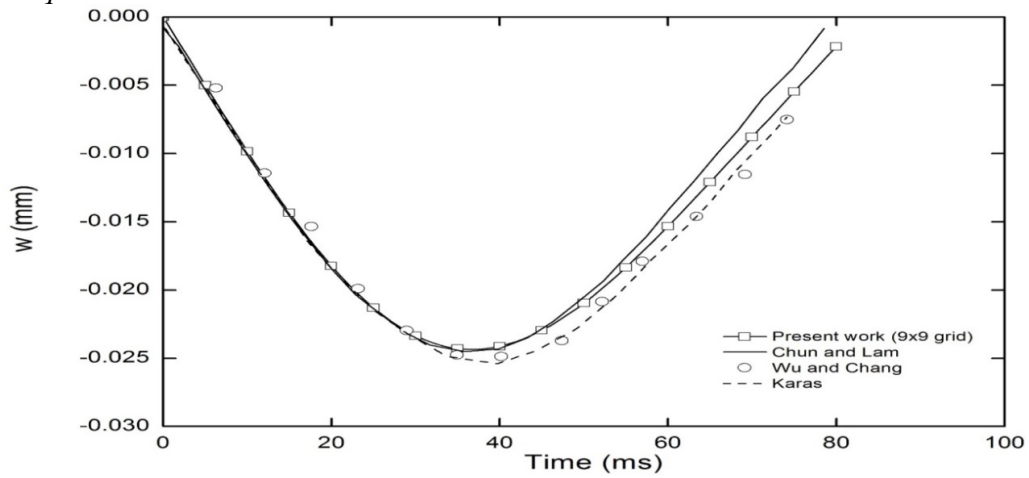
Figure 7. Comparison of displacement of the ımpactor at the contact point
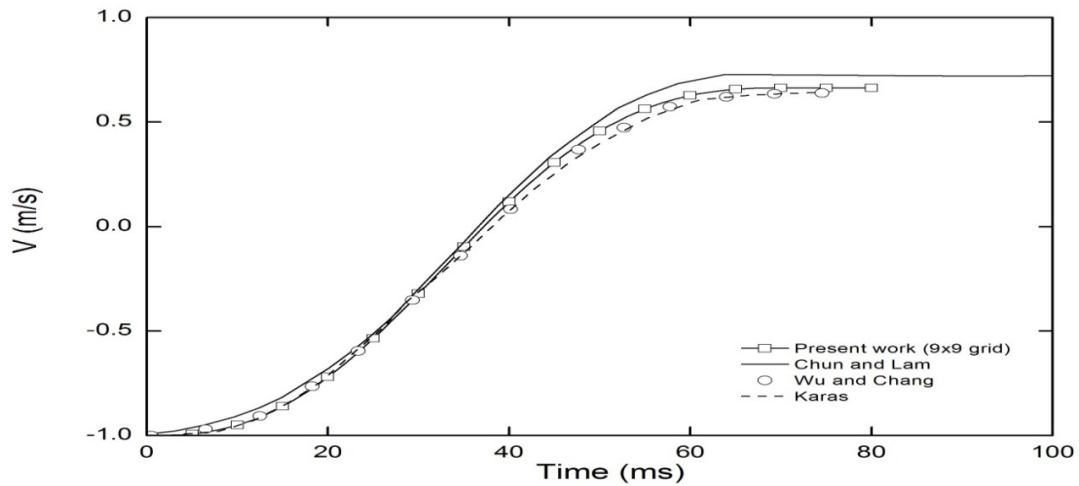
Figure 8. Comparison of ımpactor velocity

5.2. Composite plate impact problem

5.2.1 Small displacement example

In this example, a laminated composite plate is impacted by a steel sphere. Plate is clamped at all edges. Composite plate dimensions are: a=0.14 m, b=0.14 m and thickness h=0.00381 m. Two different stacking schemes are considered: cross ply of $[0^o/90^o/0^o]$ and angle ply of $[30^o/-30^o/30^o]$ layer orientations. All layers have equal thicknesses. Composite material properties are: E_1=142.73 GPa, E_2=13.79 GPa, G_{12}=4.64 GPa, ρ=1610 kg/m³, v_{12}=0.30. Material properties of steel ball are: E=206 GPa, G=79.85 GPa, v=0.28, ρ=7833 kg/m³. Mass and initial velocity of steel ball is given as m_i=0.014175 g and V_0=-22.6 m/s respectively. Contact stiffness is taken as k=1x10⁸ N/m^{1.5}.

Dynamic equations are solved with GDQ method using time step value of Δt=1 μs. Contact force, transverse displacements and velocities of the plate and ball are compared with those in the literature as shown in Figs. 9-14 [7]. In Figs. 9-14 Chun and Lam employ mode shapes and transformation of principal in obtaining solution. They use 49 terms in each direction in series expansion

to converge the solution. From Figs. 9-14, it is seen that composite plate impact results obtained with 9x9 GDQ mesh grid for cross ply and angle ply lamination schemes match to the literature very well both in character and value.
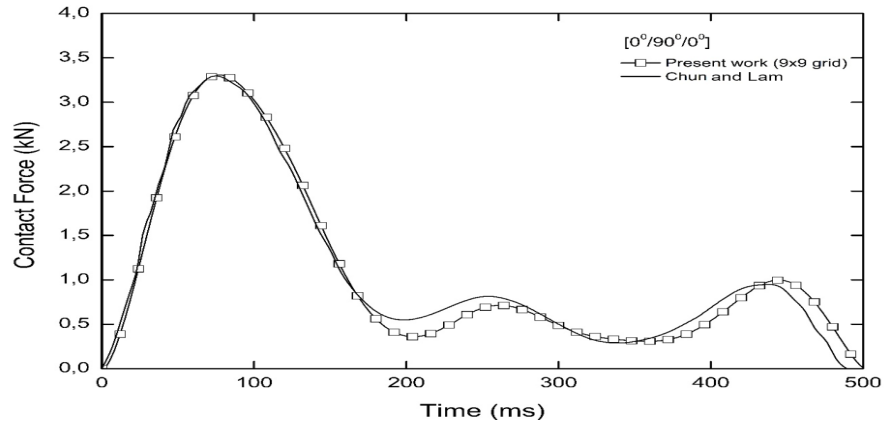
Figure 9. Contact force history for $[0^0/90^0/0^0]$ layer angles
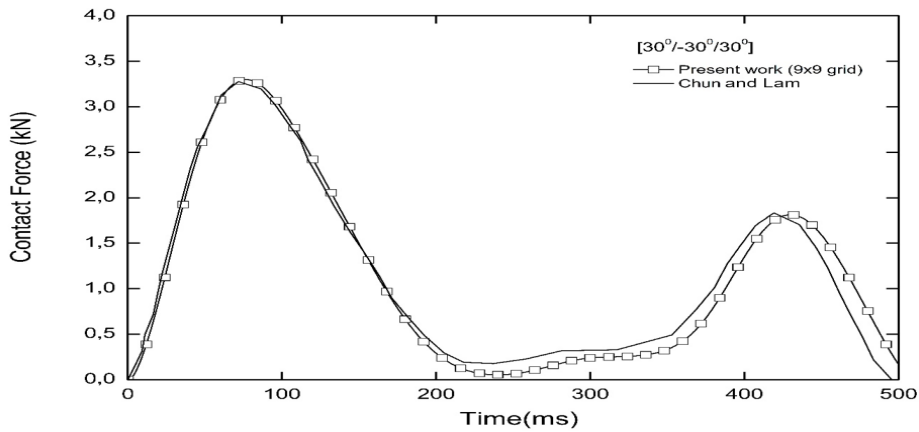
Figure 10. Contact force history for $[30^0/-30^0/30^0]$ layer angles
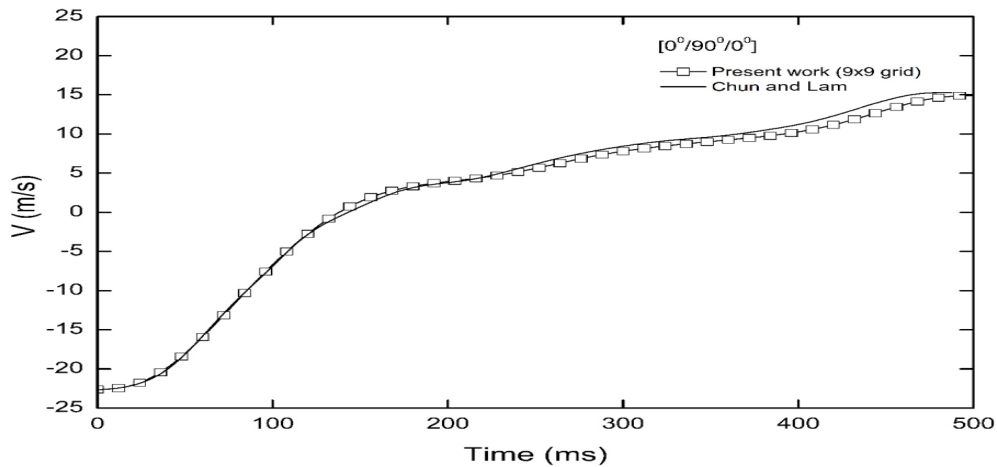
Figure 11. Impactor velocity history for $[0^0/90^0/0^0]$ layer angles
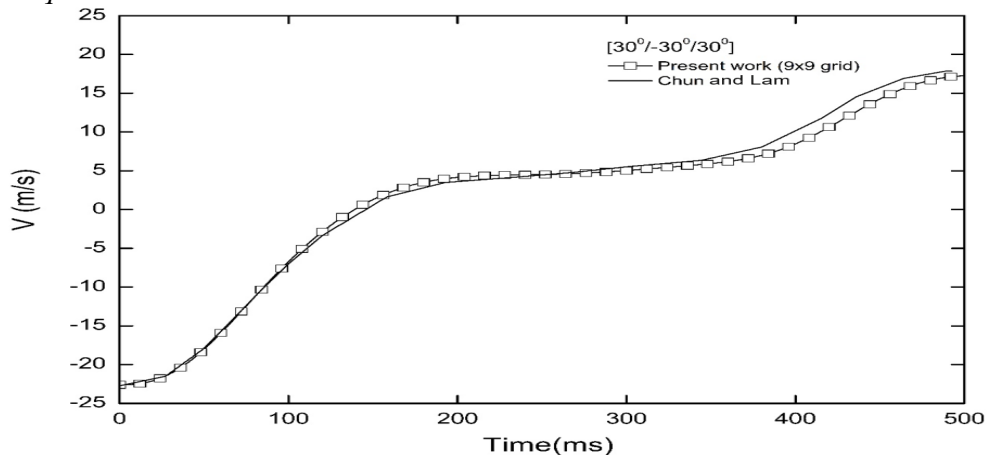
Figure 12. Impactor velocity history for $[30^0/-30^0/30^0]$ layer angles
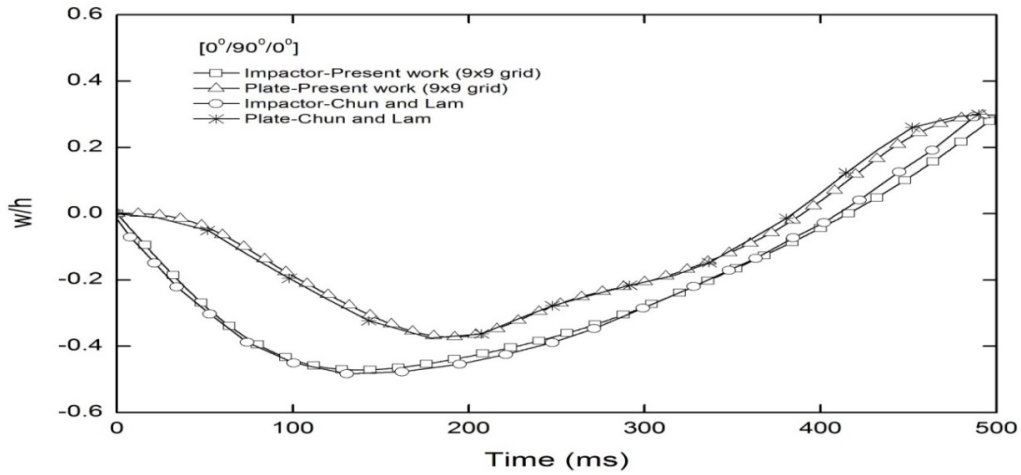
Figure 13. Impactor and plate displacement history for $[0^0/90^0/0^0]$ layer angles
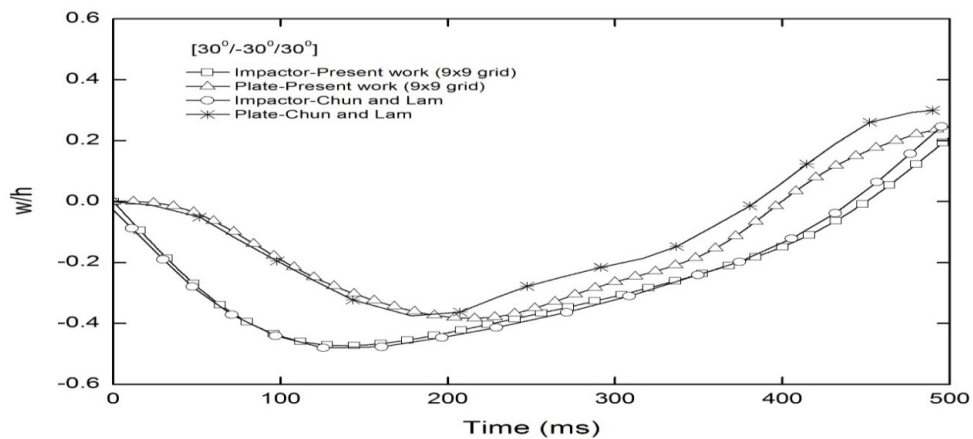
Figure 14. Impactor and plate displacement history for $[30^0/-30^0/30^0]$ layer angles

5.2.2. Large displacement example

In this example, large displacement behavior of a laminated composite plate impacted by a steel ball is analyzed. Plate is simply supported at all edges. Composite plate dimensions are: a=152.4 mm, b=101.6 mm and thickness h=2.69 mm. Stacking schemes considered is: [0/45/0/-45/0]2s. All layers have equal thicknesses. Composite material properties are: E1=120 GPa, E2=7.9 GPa, G12=5.5 GPa, ρ=1580 kg/m3, ν12=0.30. Material properties of steel ball are: E=206 GPa, G=79.85 GPa, ν12=0.28, ρ=7833 kg/m3. Mass and initial velocity of steel ball is given as mi=8.54 g, V0=-30 m/s respectively. Contact stiffness is taken as k=1.413x109 N/m1.5.

Solution of impact problem is carried out with GDQ method using the time step value of Δt=0.25 μs. Contact force, transverse displacements and velocities of plate and impactor ball are compared with the literature for large displacement case in Figs. 15-17. In Figs. 15-17, Chen and Sun [2] use 9-node isoparametric quadrilateral shell elements and they use a mesh of 8x8 shell elements.
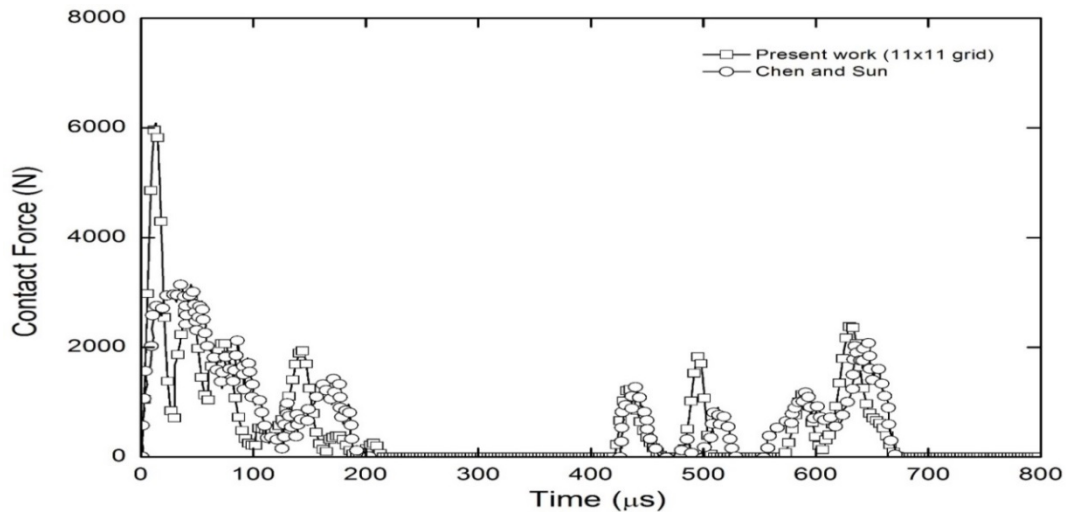
Figure 15. Contact force history for large displacement analysis
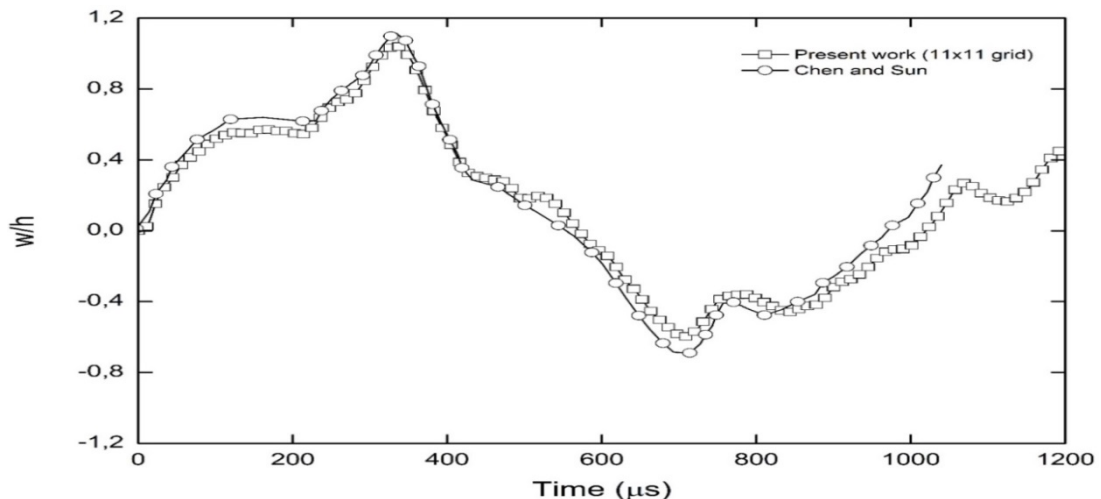
Figure 16. Transverse displacement history of the plate at ımpact point for large displacement analysis
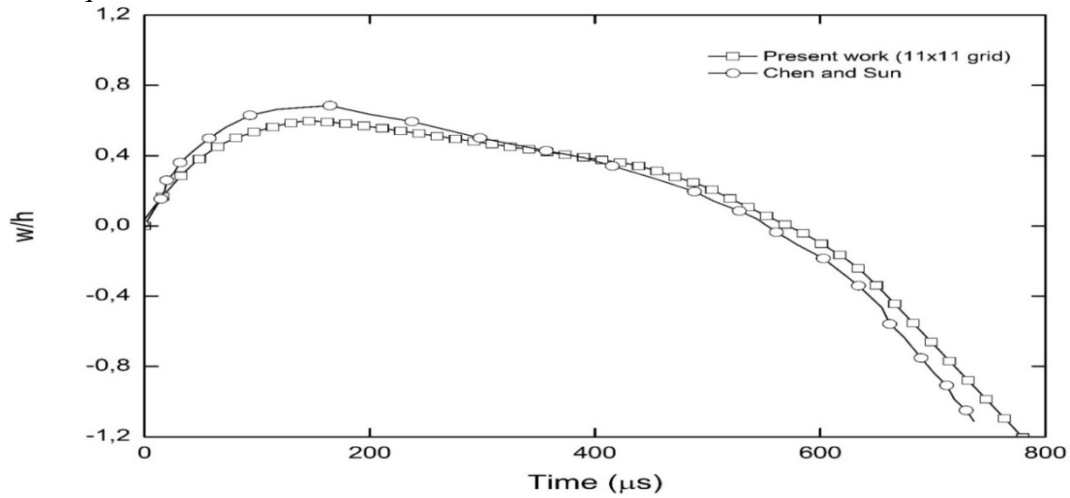
Figure 17. Displacement history of ımpactor

Figs. 15-17 show that a mesh of 11x11 grids in GDQ method can yield displacement results sufficiently close to the literature for large displacement case.

5.3.Composite cylindrical shell impact problem

5.3.1 Small displacement example

In this example, a cantilever laminated composite cylindrical panel is impacted by a steel sphere. Cylindrical panel is clamped at x=0 edge. Composite plate dimensions are: a=0.5 m, b=0.3 m, thickness h=0.005 m, R=2 m. A symmetric stacking scheme of $[0^o/90^o/0^o/90^o/0^o]_s$ layer angles is considered. All layers have equal thicknesses. Composite material properties are: E1=120 GPa, E2=7.9 GPa, G12=5.5 GPa, ρ=1580 kg/m3, ν12=0.30. Material properties of steel ball are: E=206 GPa, G=79.85 GPa, ν=0.28, ρ=7833 kg/m3. Diameter and initial velocity of impactor steel ball are given as Di=1.27 cm, V0=-3 m/s respectively. Contact stiffness is taken as k=0.811x109 N/m1.5.

Dynamic equations are solved with GDQ method using time step value of Δt=1 μs. Contact force, transverse displacements and velocities of cylindrical panel and impactor ball obtained are compared with the literature as shown in Figs. 18-21 [19]. In Figs. 18-21, Rout and Karmakar use 8-noded isoparametric shell elements in obtaining solutions. They use a mesh of 8x8 8-noded isoparametric shell elements in predicting responses.
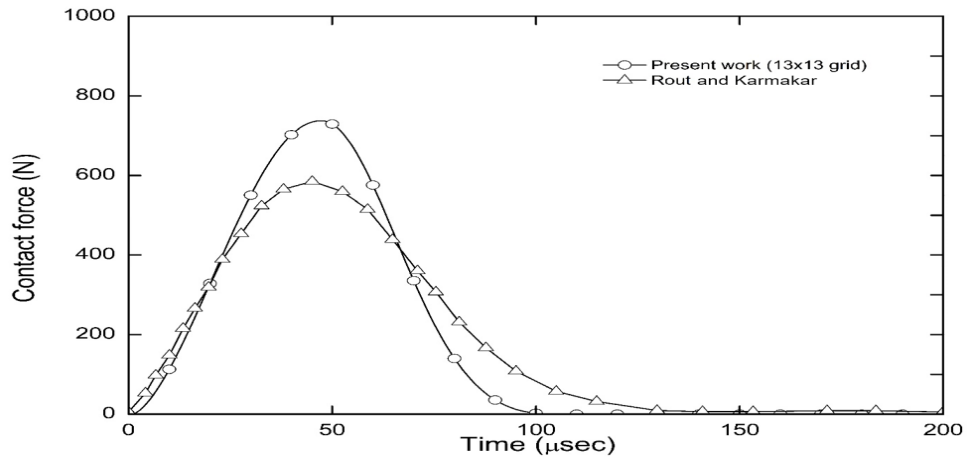
Figure 18. Contact force history
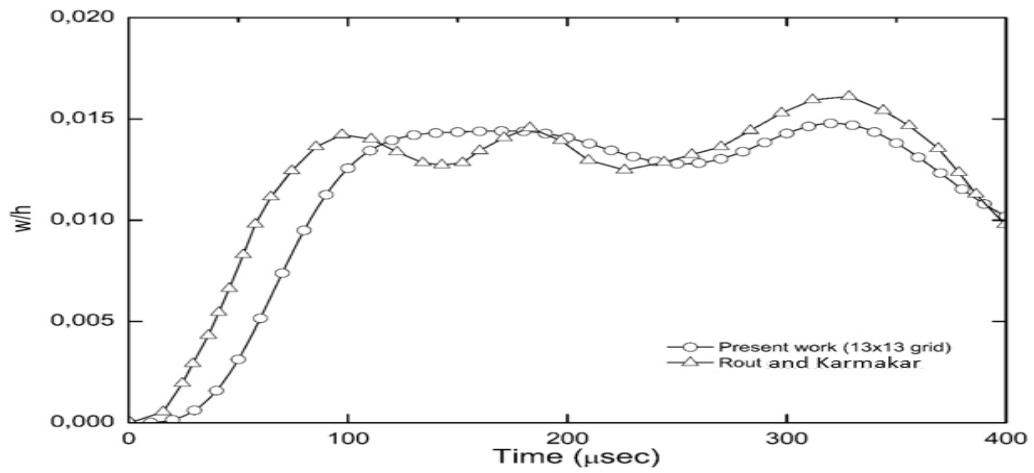
Figure 19. Transverse displacement history of cylindrical panel at ımpact point
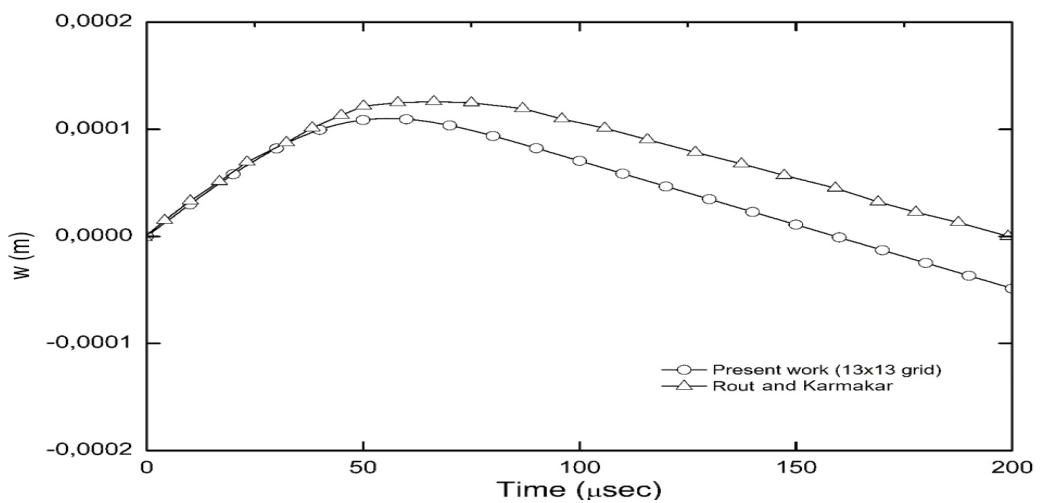
Figure 20. Displacement history of ımpactor
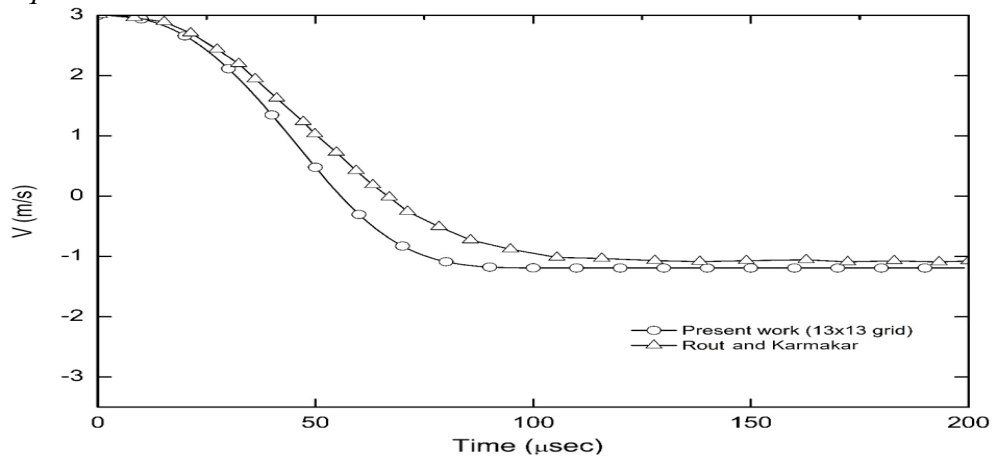
Figure 21. Velocity history of ımpactor

From Fig. 18, it is seen that the character of contact force history is quite similar with the literature. Also, the time where peak contact force occurs is in very good agreement with Rout el al. However, there is a difference in peak contact force value. From Figs 19-21, it is observed that displacement and velocity results obtained with 13X13 GDQ mesh grid for cylindrical panel and impactor ball are sufficiently close to the literature both in character and value.

5.3.2. Large displacement example

In this example, large displacement behavior of a glass/epoxy laminated composite cylindrical panel impacted by a blunt-ended steel cylinder of nose radius 5 mm is analyzed. Shell is clamped at all edges. Cylindrical panel dimensions are: $a=b=300$ mm, ply thickness $h=0.14224$ mm and with curvature $R=10a$. Stacking schemes considered is: $[90_4/0_8/90_4]$. All layers have equal thicknesses. Composite material properties are: $E_1=156$ GPa, $E_2= E_3=9.09$ GPa, $G_{12}= G_{13}=6.96$ GPa, $G_{23}=3.24$ GPa, $\rho=1540$ kg/m^3, $v_{12}= v_{13}=0.228$, $v_{23}=0.4$. Impactor has a mass of 300 g. Material properties of impactor are: E=206 GPa, G=79.85 GPa, v=0.28, ρ=7960 kg/m3. Impactor has a mass of m_i=300 g and initial velocity of V_0=-7 m/s.

Dynamic equations are solved with GDQ method using time step value of Δt=1 µs. Displacement results of cylindrical panel and impactor ball obtained are compared with the literature as shown in Figs. 22-23 [14]. In Figs. 22-23, Kumar uses FEM in obtaining responses. From Figs. 22-23, it is seen that displacement results obtained with 9x9 GDQ mesh grid for impactor and cylindrical panel are sufficiently close to the literature both in character and value.
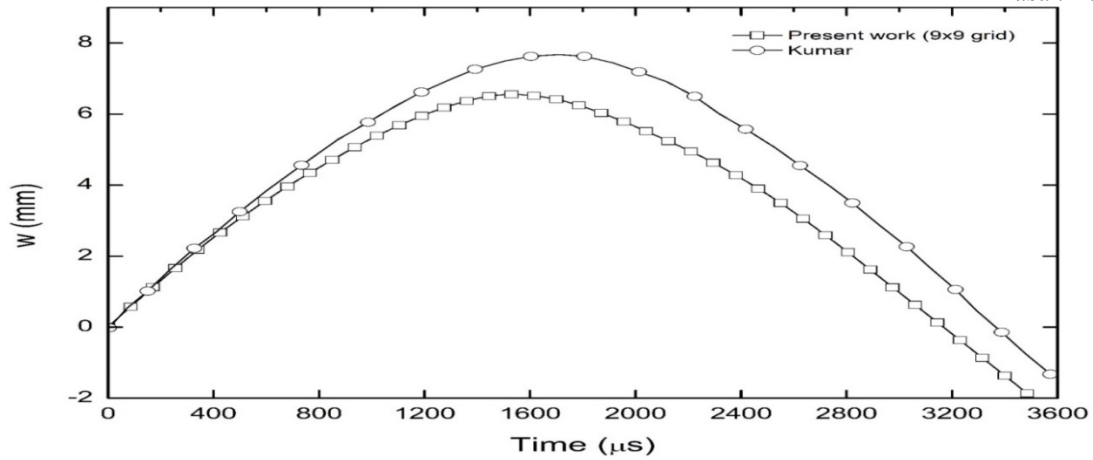
Figure 22. Displacement history of ımpactor
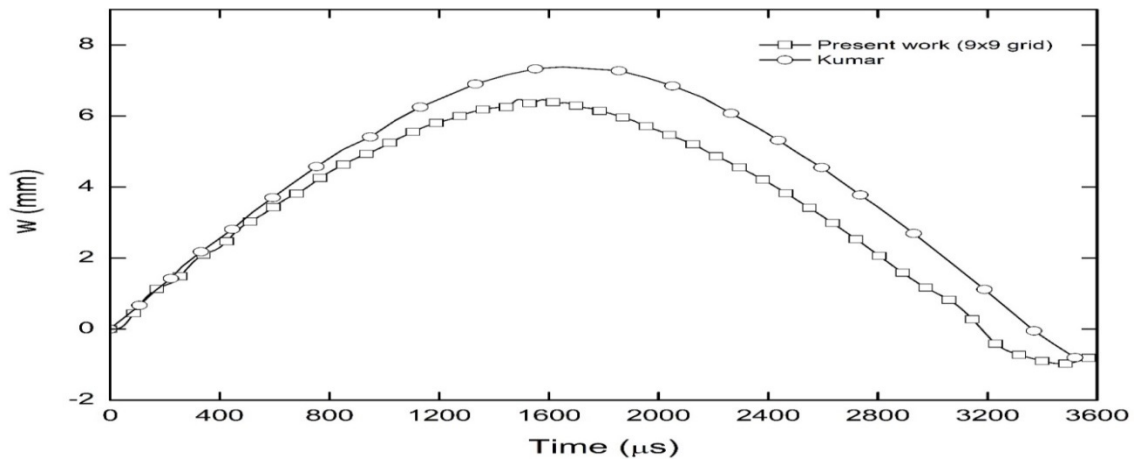
Figure 23. Central deflection history of cylindrical panel with $[90_4/0_8/90_4]$ layer angles

6. Conclusions

Contact-impact problems in mechanics are usually considered difficult to solve. In this study, GDQ method was applied to the efficient solution of low-velocity contact-impact problems of laminated composite plates and shells. Laminated composite plate and shell examples from the literature were solved using GDQ method for different boundary conditions and results were compared. Good agreement with the literature was observed for contact force, displacement and velocity results using only limited number of grids in axis directions. Slight differences in results can be attributed to the differences in the theory of solution methods as well as in plate and shell theories. Findings of this study indicate that GDQ method is an efficient tool in solving low-velocity contact-impact problems. Therefore, it can be further applied to the efficient solution of other impact problems with different shell geometries.

References

[1]Karas, K. (1939). Platten unter seitlichen stoss. Ingenieur Archiv, 10, 237-250. doi:10.1007/bf02084907

Low-velocity impact analysis of laminated composite plates and shells with generalized differential quadrature method

[2] Chen, J.K., Sun, C. T. (1985). Dynamic large deflection response of composite laminates subjected to impact. Composite Structures, 4(1), 59-73. doi: 10.1016/0263-8223(85)90020-0

[3] Sun, C. T., Chen, J. K. (1985). On the Impact of Initially Stressed Composite Laminates. Journal of Composite Materials, 19(6), 490-504. doi:10.1177/002199838501900601

[4] Wu, H.-Y. T., Chang, F.-K. (1989). Transient dynamic analysis of laminated composite plates subjected to transverse impact. Computers & Structures, 31(3), 453-466. doi: 10.1016/0045-7949(89)90393-3

[5] Cairns, D. S., Lagace, P. A. (1989). Transient response of graphite/epoxy and kevlar/epoxy laminates subjected to impact. AIAA Journal, 27(11), 1590-1596. doi: 10.2514/3.10306

[6] Liou, W. J. (1997). Impact analysis of laminated composite plates with statical indentation laws. Computers & Structures, 62 (5), 817-829. doi: 10.1016/S0045-7949(96)00317-3

[7] Chun, L., Lam, K. Y. (1998). Dynamic response of fully-clamped laminated composite plates subjected to low-velocity impact of a mass. International Journal of Solids and Structures, 35(11), 963-979. doi: 10.1016/S0020-7683(96)00231-4

[8] Vaziri, R., Quan, X., Olson, M. D. (1996). Impact analysis of laminated composite plates and shells by super finite elements. International Journal of Impact Engineering, 18(7), 765-782.

  doi: 10.1016/S0734-743X(96)00030-9

[9] Karmakar, A., Sinha, P. K. (1998). Finite element transient dynamic analysis of laminated composite pretwisted rotating plates subjected to impact. International Journal of Crashworthiness, 3 (4), 379-392. doi: 10.1533/cras.1998.0085

[10] Her, S.-C., Liang, Y. C. (2004). The finite element analysis of composite laminates and shell structures subjected to low velocity impact. Composite Structures, 66(1–4), 277-285. doi: 10.1016/j.compstruct.2004.04.049

[11] Choi, I. H., Lim, C. H. (2004). Low-velocity impact analysis of composite laminates using linearized contact law. Composite Structures, 66(1–4), 125-132. doi: 10.1016/j.compstruct.2004.04.030

[12] Karmakar, A., Kishimoto, K. (2006). Transient dynamic response of delaminated composite rotating shallow shells subjected to impact. Shock and Vibration, 13(6), 619-628. doi: 10.1155/2006/645949

[13] Tiberkak, R., Bachene, M., Rechak, S., Necib, B. (2008). Damage prediction in composite plates subjected to low velocity impact. Composite Structures, 83(1), 73-82. doi: 10.1016/j.compstruct.2007.03.007

[14] Kumar, S. (2008). Analysis of impact response and damage in laminated composite shell involving large deformation and material degradation. Journal of Mechanics of Materials and Structures, 3(9), 1741-1756.

[15] Khalili S. M. R., Soroush M., Davar A., Rahmani O. (2011). Finite element modeling of low-velocity impact on laminated composite plates and cylindrical shells. Composite Structures, 93(5), 1363–1375. doi: 10.1016/j.compstruct.2010.10.003

[16] Dey, S., Karmakar, A. (2014). Effect of oblique angle on low velocity impact response of delaminated composite conical shells. Proceedings of the Institution of Mechanical Engineers, Part C: Journal of Mechanical Engineering Science, 228(15), 2663-2677. doi: 10.1177/0954406214521799

[17] Park, H. (2017). Investigation on low velocity impact behavior between graphite/epoxy composite and steel plate. Composite Structures, 171, 126-130. doi: 10.1016/j.compstruct.2017.03.032

[18] Mao, Y., Hong, L., Ai, S., Fu, H., Chen, C. (2017). Dynamic Response and Damage Analysis of Fiber-Reinforced Composite Laminated plates under low-velocity oblique impact. Nonlinear Dynamics, 87(3), 1511-1530. doi: 10.1007/s11071-016-3130-5

[19] Rout, M., Karmakar, A. (2017). Low velocity impact performance of delaminated composite stiffened shell. Procedia Engineering, 173, 306-313.doi: 10.1016/j.proeng.2016.12.021

[20] Serge, A. (2005). Impact on composite structures. Cambridge University Press, Cambridge..

[21] Bellman, R., Casti, J. (1971). Differential quadrature and long-term integration. Journal of Mathematical Analysis and Applications, 34(2), 235-238. doi: 10.1016/0022-247X(71)90110-7

[22] Bellman, R., Kashef, B. G., Casti, J. (1972). Differential quadrature: A technique for the rapid solution of nonlinear partial differential equations. Journal of Computational Physics, 10(1), 40-52. doi: 10.1016/0021-9991(72)90089-7

[23] Shu, C. (2000). Differential quadrature and its applications in engineering, Springer-Verlag, Great Britain.

[24] Bert, C. W., Malik, M. (1996). Differential quadrature method in computational mechanics: A review. Applied Mechanics Reviews, 49(1), 1-28. doi: 10.1115/1.3101882

[25] Chen, C.N. (2006). Discrete element analysis methods of generic differential quadratures. Springer, The Netherlands.

[26] Tornabene, F., Fantuzzi, N., Ubertini, F., Viola, E. (2015). Strong formulation finite element method based on differential quadrature: A survey. Applied Mechanics Reviews, 67(2), 020801. doi: 10.1115/1.4028859

[27] Zong, Z., Zhang, Y. (2009). Advanced differential quadrature methods. CRC Press.

[28] Hong, C. C. (2010). Transient responses of magnetostrictive plates by using the GDQ method. European Journal of Mechanics - A/Solids, 29(6), 1015-1021. doi: 10.1016/j.euromechsol.2010.07.007

[29] Kurtaran, H. (2015). Large displacement static and transient analysis of functionally graded deep curved beams with generalized differential quadrature method. Composite Structures, 131, 821-831. doi: 10.1016/j.compstruct.2015.06.024

[30] Kurtaran, H. (2015). Geometrically nonlinear transient analysis of thick deep composite curved beams with generalized differential quadrature method. Composite Structures, 128, 241-250. doi: 10.1016/j.compstruct.2015.03.060

[31] Kurtaran, H. (2015). Geometrically nonlinear transient analysis of moderately thick laminated composite shallow shells with generalized differential quadrature method. Composite Structures, 125, 605-614. doi: 10.1016/j.compstruct.2015.02.045

Low-velocity impact analysis of laminated composite plates and shells with generalized differential quadrature method

[32] Civalek, Ö. (2005). Geometrically nonlinear dynamic analysis of doubly curved ısotropic shells resting on elastic foundation by a combination of harmonic differential quadrature-finite difference methods. International Journal of Pressure Vessels and Piping, 82(6), 470-479. doi: 10.1016/j.ijpvp.2004.12.003

[33] Civalek, Ö. (2007). Nonlinear analysis of thin rectangular plates on winkler–pasternak elastic foundations by DSC–HDQ methods. Applied Mathematical Modelling, 31(3), 606-624.

doi: 10.1016/j.apm.2005.11.023

[34] Viola, E., Miniaci, M., Fantuzzi, N., Marzani, A. (2014). Vibration analysis of multi-stepped and multi-damaged parabolic arches using GDQ. Curved and Layered Structures, 2(1), 28-49. doi: 10.1515/cls-2015-0003

[35] Xing, Y., Liu, B. (2009). High-accuracy differential quadrature finite element method and its application to free vibrations of thin plate with curvilinear domain. International Journal for Numerical Methods in Engineering, 80(13), 1718-1742. doi: 10.1002/nme.2685

[36] Reddy, J. N. (2003). Mechanics of laminated composite plates and shells: theory and analysis, CRC Press.